2022 IEEE 2nd International Maghreb Meeting of the Conference on Sciences and Techniques of Automatic Control and Computer Engineering (MI-STA) | 978-1-6654-7918-9/22/$31.00 ©2022 IEEE | DOI: 10.1109/MI-STA54861.2022.9837688

Performance Analysis of a Phase-Locked-Loop-based Synchronization Technique for Grid Connected-Photovoltaic Systems

Kalunga D. Mulembo
EECE Department
Cape Peninsula University of Technology
Cape Town, South Africa
mulembodesire@gmail.com

Ali Almaktoof
EECE Department
Cape Peninsula University of Technology
Cape Town, South Africa
almaktoofa@cput.ac.za

Mohamed K. Elmezughi
EECE Department
University of KwaZulu-Natal
Durban, South Africa
m.k.elmezughi@gmail.com

Abdurazag M. Khalat
EEE Department
Sabratha University
Sabratha, Libya
A.khalat@sabu.edu.ly

Shaheen Solwa
EECE Department
University of KwaZulu-Natal
Durban, South Africa
shaheensolwa786@gmail.com

***Abstract*—In recent years, the use of renewable energy systems (RESs) has become very important due to environmental concerns and the increased demand for energy. Using RESs can substantially reduce harmful emissions from polluting the environment while also offering inexhaustible resources of primary energy. Photovoltaic (PV) system has become the most common source type for residential applications or grid-connected REs. This study aims to present a power synchronization of two different power sources, namely PV system and the utility grid. A developed maximum power point tracking (MPPT) algorithm is proposed to drive the switching element of the DC-DC boost converter to accomplish fast maximum power point and maintain the voltage constant irrespective of solar radiation variation—the proper speed control to extract maximum power [1]. The proposed system provides an efficient way for power synchronization to take place. The study focuses on performance evaluation and control technique of the integration of PV system into the utility grid by means of interchangeable frequencies and voltages of the PV system with the grid, to synchronize an alternating current output of the systems injection into the grid by using the phase-locked loop synchronization technique (PLL) as the proposed method described and simulated by the MATLAB/Simulink.**

Keywords*—*PV system, phase-locked loop synchronization technique, DC-DC Boost Converter, DC-AC inverter, LCL filter.

I. Introduction

Energy is at the core of human civilization. Achievements made by humanity using energy have been exceptional, to say the least. Society has harnessed the power of two primary energy sources, namely, renewable energies and non-renewable energies, respectively. Non-renewable energy is derived from earthly resources such as fossil fuels. This poses a significant disadvantage because of the scarcity humans face today for harnessing fossil fuels due to their limited supply. In South Africa alone, 92% of its non-renewable energy sources are derived from fossil fuels such as coal, gas, and oil [1], [2]. These emit harmful greenhouse gases such as carbon dioxide into the atmosphere, leading to a rise in climate change.

Renewable energy sources – on the other hand – play a massive role in this constrained non-renewable energy source world. These take the forms of wind power (onshore and offshore), solar power from the sun, hydropower, and biomass energy from dead plants and animals. Although some argue that renewable energy sources often mislead governments, the pros outweigh the cons [3]. Renewable energy sources can produce an unlimited supply of power over the long term, but they are limited by the hardware available. As such, academics and industry professionals have switched focus to combining two or more renewable energy hardware to produce a more efficient, self-sustaining solution.

One such renewable energy case is the photovoltaic (PV) cell which harnesses the power of the ultra-violet rays from the sun and converts it to human-usable power. Unfortunately, PV cells have seen tremendous uphill growth in adopting its methodology. Older PV cell models need to be isolated and connected to the grid, but with recent advancements in technology, the new PV cells no longer need isolation, but they can be integrated into the grid utilizing electric generation injecting (EGI). EGI is injecting energy generated by renewable sources into the primary electricity grid.

One way in which EGI can be achieved is by utilizing a grid-connected energy system (GCES) via renewable sources. GCESs allow for powering of space using naturally occurring phenomena such as the sun, wind, and hydrolysis. The extra energy produced by the GCES is passed back into the grid, which helps keep the power on while the natural sources are not available. This provides an advantage because it eliminates the expense of large energy storage systems such as generators.

In this article, the authors look at how a distributed generation using PV cells can affect the operation of a national electricity grid whose design was built for a centralized generation. This is highly beneficial to countries like South Africa, which have electricity grids with a similar design.

II. NETWORK DESIGN SYSTEM MODEL

This section introduced the methodology and procedures used for the synchronized system and provided justifications for selecting each component. Fig. 1 illustrates the PV block

978-1-6654-7918-9/22/$31.00 ©2022 IEEE

diagram connected to an entire grid. In figure 1, the PV array is connected to the DC-DC converter, which converts the energy from the PV array to a smooth boosted DC voltage. The output of the DC-DC converter is then fed into an inverter (DC-AC converter) that converts the smoothened DC voltage into an AC voltage that can be used. This is then fed directly into the grid.

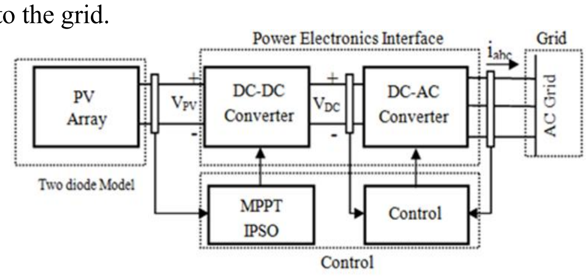

Fig. 1. A full grid connected PV Block Diagram.

A. *The PV Sizing Specification*

This study collects environmental data such as temperature and solar radiation to forecast the PV system performance. The location that the data was collected from is known for the abundance of solar radiation. In Figure 2 a monthly average of radiation and temperature for the year 2020, the average temperature was 21.2°C and a radiation average of 1834.4 kWh.m^2 [4], [5].

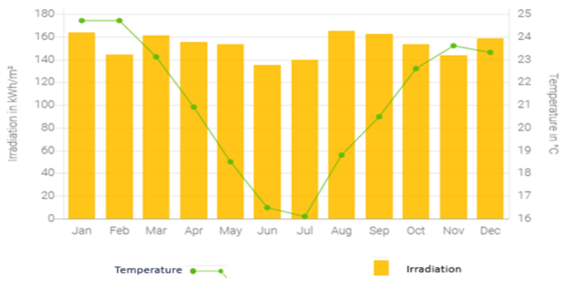

Fig. 2. The histogram of the monthly average of radiation and temperature.

From Fig. 2, the PV system components consider the following parameters: i) average solar energy intensity on horizontal surfaces, radiation in South Africa is ranging from 4.5 to 6.6 kWh/m^2 per day, which corresponds to average peak sunshine hours PSH = 8h/day [4] and ii) the daily average energy consumption of a residential house or one public or private utility; such an amount of energy represents in average the consumption of a considerable percentage of residential houses and small private or public foundations in the selected site [6] . Hence, the PV array peak power (PPV) is obtained from (1) as:

$$P_{PV} = \frac{E_d}{PSH*\eta_{CR}*\eta_{Inv}}. \quad (1)$$

In (1), E_d is the daily energy consumption of the residential house in kWh/ day, PSH is the peak sunshine hours measured in hours/ day, η_{CR} is the charge regulator efficiency and η_{Inv} is the inverter efficiency. The characteristics of PV solar module that was selected for the study is shown in Table I.

In the literature, different sizes of the PV modules produce different amounts of power. In order to determine the size of the PV module, the total peak wattage produced is needed. The system can be designed with the PV modules in series or parallel. Hence, to calculate the number of PV panels needed, we perform the following mathematical operations:

The energy required to cover the PV array is determined as:

$$P_{required} = \frac{P_{load}}{\eta_{inverter}}. \quad (2)$$

In (2), $P_{required}$ is the required energy needed to cover the PV array, P_{load} is the total load of the house or building in watt-hours (Wh) and $\eta_{inverter}$ is the efficiency of the inverter. The second step is to determine the modules' energy output per day:

$$P_{module} = P_{max} \times t_{peak}, \quad (3)$$

where P_{module} is the PV modules' energy output per day and t_{peak} is the average daily peak sunshine hours. The third step is determining the number of modules needed for the power that is injected into the grid:

$$\eta_{pv} = \frac{P_{array}}{P_{module}}. \quad (4)$$

In (4), η_{pv} is the number of PV modules needed, P_{array} is the output of the PV array in Wh and P_{module} is the output of one PV module in Wh. Finally, step four requires the determination of the number of strings connected in parallel:

$$n_{parallel} = \frac{n_{pv}}{n_{series}}. \quad (5)$$

In (5), $n_{parallel}$ is the number of PV strings that are required to be connected in parallel and n_{pv} is the total number of PV modules needed.

Table I: Sinetech AEG AS-PS07 Module Specifications

Parameter	Value
Cells	Polycrystalline solar cell
No. of cells and connections	60 (6X10)
Module dimension	1640 mm x 992 mm x 40 mm
Maximum power, P_{max}	213.15W
Rated voltage at P_{max}, V	29V
Current at P_{max}, I_{mp}	7.35A
Open-circuit voltage, V_{oc}	36.3A
Short circuit current, I_{sc}	7.84A
Temperature coefficient	-0.36 %/°C
Operating temperature	-40°C to 85°C

B. *Design of the DC-DC Boost Converter*

The equivalent circuit of a DC-DC boost converter fed by PV generation panels is depicted in Fig. 3. The boost converter is employed because the output voltage of the PV cell is low. Hence, the voltage is ramped up from a low voltage to an output voltage value of between 350V_{DC} to 600V_{DC}.

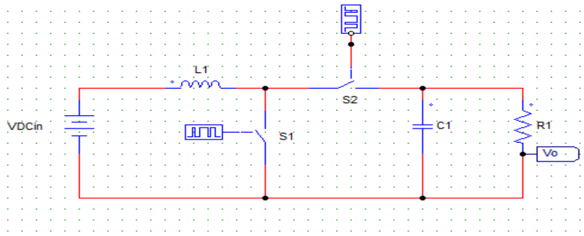

Fig. 3. A basic illustration of the boost DC-DC circuit.

To calculate the inductor and capacitor values for the application. A boost converter was designed for continuous-current operation and have an inductor value greater than the minimum inductance (L_{min}). The minimum inductance for continuous current in the boost converter is given as:

$$L_{min} = \frac{D(1-D)^2 R}{2 f_{sw}}, \tag{6}$$

where, D is the duty ratio, f_{sw} is the switching frequency, R is the resistor of the boost converter and V_o is the output voltage. The inductance L can be expressed in terms of a desired variation in the inductor current Δi_L as [7]:

$$L = \frac{V_S DT}{\Delta i_L} = \frac{V_S D}{\Delta i_L f_{sw}}, \tag{7}$$

where, Δ_{i_L} is current ripple, V_s is the input voltage. The peak-to-peak voltage ripple (ΔV_O) can be evaluated from the capacitor current. The variation in capacitor voltage can be determined as:

$$\frac{\Delta V_O}{V_O} = \frac{D}{RCf_{sw}}. \tag{8}$$

Therefore, the capacitance can be expressed in terms of voltage ripples as:

$$c = \frac{D}{R(\Delta V_O / V_O) f}. \tag{9}$$

The flowchart of the developed a maximum power point tracking (MPPT) algorithm is shown in Fig. 4. The proposed control algorithm ensures proper speed control to extract maximum power. The PVs operating voltage is perturbed by a small increase of dV, resulting in a change dP. If dP is positive, the operating voltage's perturbation is kept in a similar direction as the small increase. In contrast, if dP is negative, the operating point shifts away from the maximum power point, and the operating voltage must shift in the opposite direction of the small increase.

The algorithm considers the voltage measurements $V(k)$ and the current measurements $I[k]$ at a predetermined time interval, referred to as the MPPT period. This time span governs how often the algorithm decides to vary the system operating point. Subsequently, the algorithm assesses the power $P[k]$, the variation in power ΔP, and voltage ΔV. The ΔP and ΔV values are determined by using the measurements at the present instant $V(k)$ and $I(k)$ as well as the previous measurements $V(k-1)$ and $I(k-1)$. Then, the algorithm uses basic logic to decide what to do. The ΔP and ΔV values are each compared against zero to determine if they have risen or dropped [8]–[10].

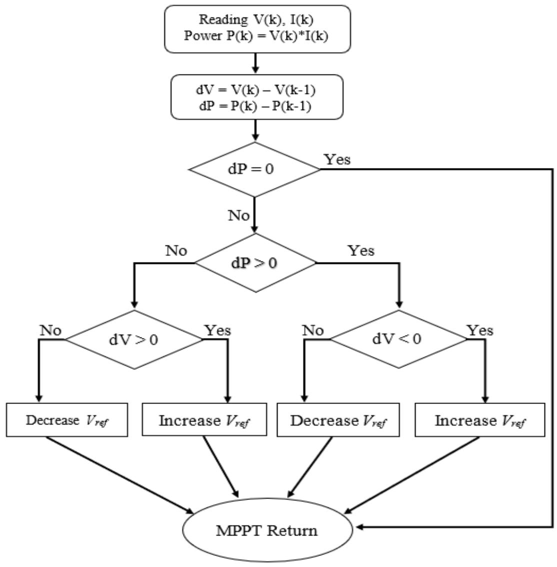

Fig. 4. Flowchart of MPPT algorithm for PVs with a boost converter.

C. Grid-Connected Inverter Design

A current control of grid-connected inverter together with the PWM scheme is used to ensure that the inductance current tracks the sinusoidal reference current closely [11]–[13]. For the design of this inverter, the authors had selected the switching frequency as f_{sw} = 10 KHz. Hence, the resonance frequency can be calculated such that:

$$f_{res} = \frac{f_{sw}}{10}. \tag{10}$$

In (10), f_{sw} is the switching frequency and f_{res} is the resonance frequency respectively. In Fig. 5, the current control method of the inverter together with the PWM scheme is illustrated for the three-phase full bridge inverter. The switch is turned on or off depending on the modulation scheme used to obtain the sinusoidal output[8], [14].

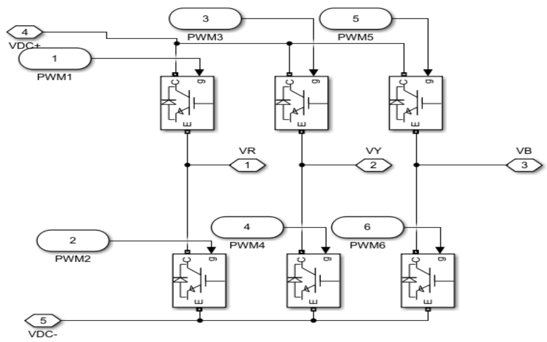

Fig. 5. The current control method of two-level inverter with PWM switching

D. LCL Filter Design

LCL filter are designed and placed between the inverter and the grid to attenuate or filter the switching frequency harmonics produced by the inverter [14], [15]. The formula used to calculate LCL filter at the inverter side is given as:

$$L_i = \frac{V_{DC}}{16*f_{sw}*\Delta I_{L-max}}, \quad (11)$$

where, V_{DC} is the DC link voltage, ΔI_{L-max} is the current ripple specified and f_{sw} is the switching frequency and ΔI_{L-max} is the 10% current ripple specified by:

$$\Delta I_{L-max} = 0.01 * \frac{P_n\sqrt{2}}{V_n}, \quad (12)$$

where V_n is the line to line RMS voltage (inverter output) and P_n is the rated active power. Secondly, the gird side inductance L_g can be calculated as:

$$L_g = \mathrm{r} * L_i. \quad (13)$$

Finally, the design of the filter capacity (C_f) proceeds from the fact that the maximal power factor variation acceptable by the grid is 5%. The filter capacity can therefore be calculated as multiplication of system base capacitance C_b:

$$C_f = 0.05 * C_b, \quad (14)$$

where $C_b = \frac{S}{V^2*2\pi*f}$. The value of the damping resistor R_{sd} can be calculated as:

$$R_{sd} = \frac{1}{3w_{res}*C_f}. \quad (15)$$

III. CONTROL SYSTEM FOR THE GRID CONNECTION

There are many challenges that are experienced when integrating solar systems with the main grid directly. For this reason, a special control circuit is needed for synchronization. When interfacing the solar system with the main grid, synchronization will only occur and be maintained when the grid parameters (voltage, current, phase and frequency) match those of the inverter. In the literature, there are many different methods that can be employed to solve the synchronization. Choosing the best method is directly dependent on the characteristics of the source. For this paper, the authors use the method of phase locked loop (PLL) due to have two different source energies respectively.

The PLL system uses a feedback loop with PI-tracking for the phase angle. The input is the three phases of the grid voltage and the output of the PLL is the phase angle of one of the three phases [9], [16]. The PLL used to generate the signal and that signal used as reference for implementation controller of grid conned inverter. And when we send the reactive power to the grid we used PLL to generator a signal that is 90° out of phase with the actually voltage. The PLL structure is classified into three types: i) stationary reference frame based PLL, ii) zero crossing detection based PLL and iii) synchronously rotating reference based PLL [17]. The basic idea of the SRF PLL is a feedback system with PI regulation tracing the phase angle. the voltage signals V_A ; V_B and V_C are transferred from three phases to a stationary system of two phases V_α and V_β. The grid voltage is given as: V_A ; V_B and V_C.

In order to track the phase angle of the three phase signals, V_a, V_b and, V_c must be transferred from three phases to a stationary of two phases V_α and V_β, the grid voltage are given as:

$$V_a = Vm(sin\,\theta), \quad (16)$$
$$V_b = Vm(sin(\theta - \tfrac{2\pi}{3}), \quad (17)$$
$$V_c = Vm(\sin(\theta + \tfrac{2\pi}{3})), \quad (18)$$

In (16)-(18), θ is the phase angle calculated as $\theta = 2\pi f$. The $\alpha\beta$ transformation matrix is given as:

$$\mathrm{T}\,\alpha\beta = \frac{2}{3}\begin{vmatrix} 1 & -\frac{1}{2} & -\frac{1}{2} \\ 0 & -\frac{\sqrt{3}}{2} & \frac{\sqrt{3}}{2} \end{vmatrix}. \quad (19)$$

The matrix multiplication $V_{\alpha\beta} = \mathrm{T}\,\alpha\beta V_{abc}$ yields:

$$\begin{vmatrix} V_\beta \\ V_\alpha \end{vmatrix} = \begin{vmatrix} V_m\,(\sin\theta) \\ V_m\,(\cos\theta) \end{vmatrix}. \quad (20)$$

A. Synchronous Rotating or Transform V_α , V_β to V_q , V_d

The phase angle of V_α is tracked by the synchronization of the voltage space vector along the Q-axis or D-axis in the SRF [18], [19]. Fig. 6 illustrates the unsynchronized voltage space vector with the Q-axis and D-axis respectively.

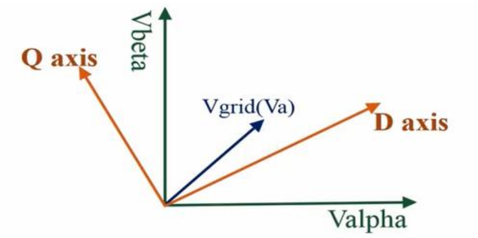

Fig. 6. The phase diagram of abc-frame to αβ-frame and αβ-frame to dq-frame not synchronous

The voltage space vector is to be synchronized with the q-axis the transformation matrix is**:**

$$\mathrm{T}qd = \begin{vmatrix} \cos\theta^* & \sin\theta^* \\ \sin\theta^* & \cos\theta^* \end{vmatrix}, \quad (21)$$

where θ^* is the estimated phase angle output of the PLL system. Carrying out the transformation $Vqd = T_{qq}V_{\alpha\beta}$ and using the trigonometric addition formulas yields:

$$\begin{vmatrix} V_d \\ V_q \end{vmatrix} = \begin{vmatrix} -V_m\,\sin(\theta - \theta^*) \\ V_m\,(\cos\theta - \theta^*) \end{vmatrix}. \quad (22)$$

The gain of the PI regulator is designed so that V_q follows the reference value $V_d{}^*= 0$, which is shown in Fig. 7. If $V_d = 0$ then the space voltage vector is synchronized along D axis and estimated frequency ω is locked on the systems frequency ω. In Fig. 7, the voltage space vector is synchronized with D-axis. The active component is aligned in phase with α and the reactive component is aligned in phase with β.

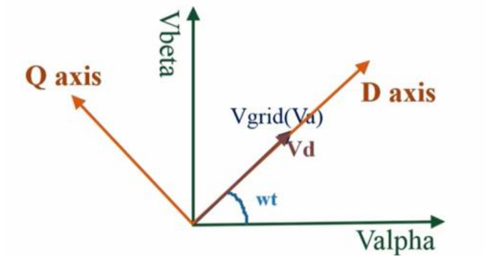

Fig. 7. The phase diagram of V_{grid} synchronous with D axis or Q axis.

To achieve a satisfactory performance and small steady state errors in magnitude and phase, the compensator design is not easy task by use method show in Fig. 8:

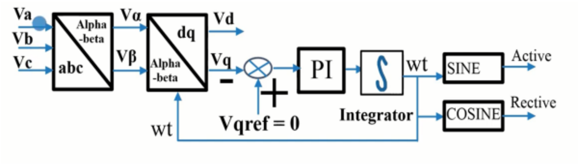

Fig. 8. The basic traction for the SRF PLL.

B. Implementation of Transfer Function

The transfer function (TF) for the plant is just a lag and an integrating element. For the plant in Fig. 8 is just a lag and integrating element [1], [19]:

$$G_p = \left(\frac{1}{1+TS}\right) * \left(\frac{1}{s}\right). \tag{23}$$

For the simulation, Ts is period for the sampling the open-loop TF for the system in Fig. 9 described as:

$$G_{ol} = \left(kp\frac{1+s\tau}{s\tau}\right) * \left(\frac{1}{1+ST}\right) * \left(\frac{Vm}{s}\right). \tag{24}$$

To go from the open-loop system to the closed-loop system the relation between the transfer functions as follows:

$$G_{cl} = \frac{G_{ol}}{1+G_{ol}}. \tag{25}$$

The most straightforward method to use for solving integration is found in [1], [20]. In reality, grid connected PV system voltage input signal for PLL system are sampled. The system has been designed to be capable to handle these signals. The integration element in the plant as follow:

$$G_{(s)} = \frac{F(s)}{E(s)} = \frac{1}{s} * \Leftrightarrow \frac{df}{dt} = \mathrm{e(t)}. \tag{26}$$

Using Euler forward by taking the mathematical expression Z-transform gives:

$$S = \frac{Z-1}{Ts}. \tag{27}$$

Using (27) the PI-regulator in the z-domain is determid as follows:

$$G_{pi} = kp\frac{1+s\tau}{s\tau} = kp\frac{z-1+\frac{Ts}{\tau}}{z-1}. \tag{28}$$

The transfer function (TF) for the PLL system in equetion (28) can be rewritten as follows:

$$G_{ol} = \left(kp\frac{1+s\tau}{s\tau}\right) * \left(\frac{1}{1+ST}\right) * \left(\frac{Vm}{s}\right) = kp\frac{z-1+\frac{Ts}{\tau}}{s^2\left(s+\frac{Ts}{\tau}\right)} = kp\frac{Vm}{aTs} * \frac{\left(\frac{a}{\tau}+as\right)}{s^2\left(s+\frac{1}{T}\right)}. \tag{29}$$

In (29), Ts is the sampling period in second, Kp is the regulator gain, $\frac{1}{1+ST}$ is the lag term of the system, $\frac{1}{s}$ is the integratting element which the depicts voltage controlled oscillator, V_m is the amplitude voltage level in volts, G_{ol} is the open loop transfer funtion and G_p is the transfer of the of the full system [21].

IV. RESULTS AND DISCUSSIONS

The PLL control method been used to synchronize the PV system with the grid, when the PV system was injected into grid using the proposed PLL synchronization technique, the frequency matched with each other, phase difference becomes zero, the resultant voltage raised to the desired range [22].

The step taken in order to achieve the synchronization process can be defined as matching the frequency, phase angle, sequence and voltage of the grid with the PV system, if the two supplies are not matching that mean are unsynchronized then injection of PV system into grid will never be done, therefore the synchronization is needed for the penetration of PV into grid to take place. In this research the PLL control method been used to synchronize the PV system with the grid, when the PV system was injected into grid using the proposed synchronization technique, the frequency matched with each other, phase difference becomes zero, the resultant voltage raised to the desired range.

The PLL has been designed and tested. At connection point of grid voltage are 400V and frequency 50Hz, the phase angle was tracked fast and accurate, and PV system has been designed to feed the grid with 100kw/h and the voltage MPPT it between 270V to 300V**.** Grid connected PV system connected with PLL in MATLAB/Simulink platform is depicted in Figure 9. The specification and parameters of the PV panels are tabulated in Table II. The DC-DC boost converter has been designed and calculated with specification shown in tables III. Table IV presents the calculated inverter and LCL filter parameters.

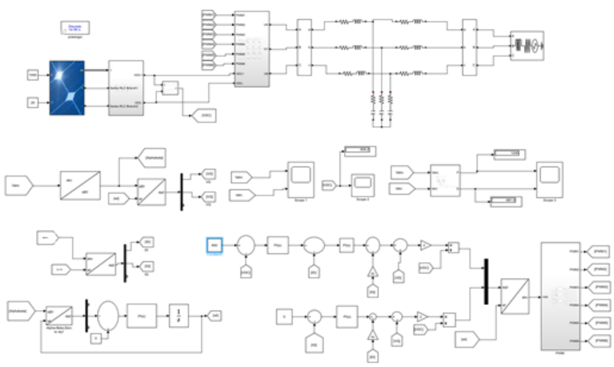

Fig. 9. Grid connected PV system connected with PLL in Simulink.

The size of the system depends on the load that it supplying, the Table II below shows the specifications parameters values of the PV systems, the number of the Panels connecting in parallel and series, the power output or generated by the PV and the voltage supplied.

Table II: The PV sizing specification.

Parameter	Value
Output Power, P	100kW
Open circuit voltage, V_{oc}	363V
MPPT voltage, V_{MPPT}	270-300 V
Total of panels, n_{pv}	470
Series modules, n_{series}	10
Parallel strings, $n_{parallel}$	47

The output voltage of solar array is varying due to the irradiance change, DC to DC boost converter was been designed to Stabilized by set up the Voltage from Solar array to be boost and fix at output of the DC to DC boost convertor where used an inductor as an energy Storage component to upkeep the output with supplementary energy in adding to the DC input source and This effects the output voltage to boost, the design specification are shown in Table III below.

Table III: Boost Converter Specification.

Parameter	Value
Rated Power, P	100kw
Switching, f_{sw}	5Khz
Input voltage, V_{in}	250-300V
I ripple	5%
V ripple	1%
Output voltage, V_{out}	600V
Inductor, L	1.458mH
Capacitor, C	3227.77uF

Three-phase full bridge inverter, has been designed as a current control method of inverter with PWM switching, the command of the switch depends on the modulation schemes to obtain the sinusoidal output. The LCL filter are designer and place between the inverter and the load so that it can reduce the Harmonics in the system, specification of the inverter and LCL are shown in Table IV below.

Table IV: Inverter and LCL Filter Specification.

Parameter	Value
Switching frequency, f_{sw}	10KHz
Capacitor, C	100uF
Inductor, $L_i = L_g$	500uH
Resistance, R	1mΩ
Grid voltage, V_{grid}	400V rms
Grid frequency, f	50Hz
Rated power, P	100kw

The first test was done when current inject into grid at the standard testing condition (STC) with constant irradiances of 1000 w/m^2 and temperature of 25°C. Figures 23, 24 and 25 show the balance grid system that been injecting with a PV current, but before the synchronized take place there is 40ms delay time. The PLL was run on step size is set to the sample period 1/2000 = 0.5ms.

Fig. 10 represents the average relative times take for PV system to synchronized with the grid, observed various simulations test cases using MATLAB/Simulink where the temperature and irradiances changed. For each simulation test average response time that take for the synchronization to be done. The results presenting in form of prediction graph where X-axis represents the times and Y-axis represents the voltages. Fig. 11 shows the output voltages of grid and PV system, by checking the X-axis and Y-axis when the two waves matched, and the simulation was run on 25°C and irradiances at 1000 w/m2.

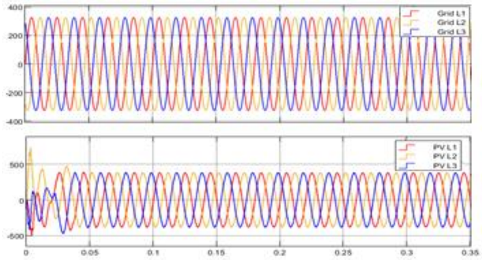

Fig. 10. V_{grid} synchronized with current inverter.

The Fig. 11 below shows that boost converter only takes 0.04s to adjust the output voltage to be stable, the X-axis represents the times, and the Y-axis represents the voltages and test was run at 25°C and irradiances at 1000 w/m2. It can be observed that the DC-link value to the inverter has been achieved from the PV panels through the boost converter at the STC values.

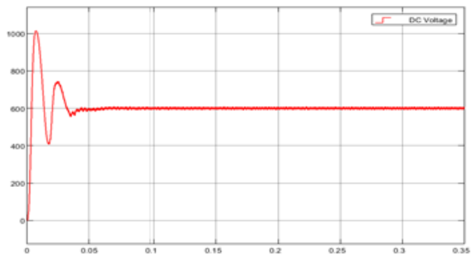

Fig. 11. V_{dc} waveform.

Fig. 12 below shows the active and relative power graphs when the irradiance and temperature at STC with irradiance of 1000 w/m2, and tempter of 25°C. From Fig. 12(a) the active power took 0.04s to be stable or synchronized and Fig. 12(b) shows the reactive power, where took almost 0.04s to be synchronized as well.

(a) Active power

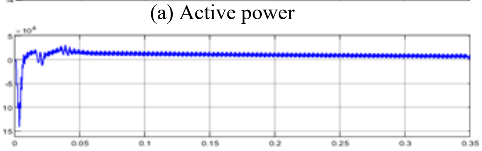

(b) Reactive power

Fig. 12. Active and reactive power waveform.

The second test was done when current inject into grid when the irradiances changes. It was found that when the irradiances increase the PV current increase and when irradiances decrease, PV current decrease as seen in Figures 13, 14 and 15. Fig. 13 shows the voltage and current of the grid with different irradiances, the test was run from 1000W/m2, 700W/m2, and 500W/m2, and the temperature was at 25°C. It has been noticed that the PV output voltage is decreased when irradiances is decreased and vice versa.

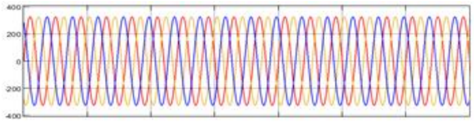

(a) Grid voltage

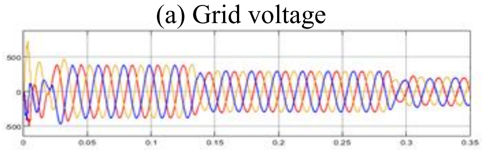

(b) PV output voltage

Fig. 13. Voltage and current waveforms with different irradiances.

Fig. 14 below every time the irradiation applied changed by increased or decrease, the Vdc voltage also apply a changed by increased or decreased in a short time. The irradiances start from 1000W/m2, 700W/m2, and 500W/m2, temperature of 25°C. The dynamic response of the system was found very fast when the radiations were changed.

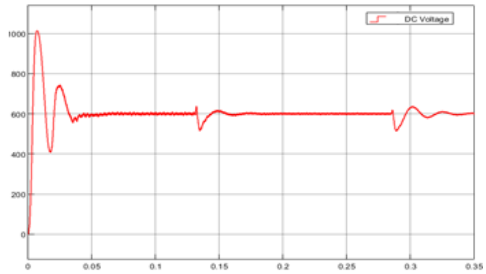

Fig. 14. DC Voltage waveform with different irradiances applied.

Fig. 15 shows the active and reactive power when the irradiances change by increased or decreased, the active and reactive power also increased or decreased for a short period of time. The test run from 1000W/m2, 700W/m2, and 500W/m2, temperature of 25°C see figure 28. Once again, the proposed control system shows a fast dynamic response to follow the changes of the radiations.

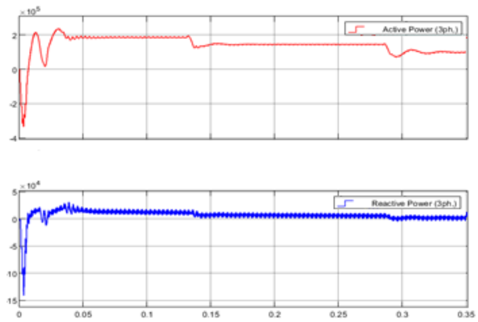

Fig. 15. Active and reactive power wave with different irradiance applied.

V. Conclusion

This paper presents a model of a grid-connected photovoltaic system for synchronization studies. The PV panel and the DC-DC boost converter, an inverter system, and an LCL filter were done. The simulation model included the simple design of the MPPT algorithm for a boost converter fed by the PV system, and PLL for grid synchronization implementation was based on MATLAB/Simulink. First of all, a developed MPPT algorithm has been proposed. The proposed technique drives the switching element of the DC-DC boost converter by modifying the converter's duty ratio and continuously tracking the maximum power point irrespective of solar radiation variation. Secondly, a PLL technique for grid synchronization implementation simulation scenarios was presented to properly understand grid-connected PV systems and the importance of using the PLL synchronization technique. The simulation shows the delay times of 40ms before the penetration of the photovoltaic current into the grid. To solve this problem, we will have to use the P&O method because the method asks how to calculate the gain; the greater the gain, the delay time also becomes small. The proposed control system shows a speedy dynamic response to follow the changes of the radiations. In general, the PLL works very well, the PI regulation works very well, and it is exact and follows the grid phase under balance grid conditions.

References

[1] S. Natesan and J. Venkatesan, “A SRF-PLL Control Scheme for DVR to Achieve Grid Synchronization and PQ Issues Mitigation in PV Fed Grid Connected System,” no. August, pp. 2996–3015, 2016.

[2] C. Bergh and B. Cohen, “Energy efficiency in the South African oil refiniing industry,” 2011 Proc. 8th Conf. Ind. Commer. Use Energy, ICUE 2011, pp. 46–52, 2011.

[3] M. J. B. Kabeyi and O. A. Olanrewaju, “Managing sustainability in electricity generation,” IEEE Int. Conf. Ind. Eng. Eng. Manag., vol. 2020-Decem, pp. 530–536, 2020, doi: 10.1109/IEEM45057.2020.9309994.

[4] N. T. Du Plooy, A. C. Brent, and I. H. De Kock, “Fostering sustainable energy transitions for South Africa’s electricity sector: A set of criteria,” 2017 IEEE Technol. Eng. Manag. Soc. Conf. TEMSCON 2017, pp. 131–136, 2017, doi: 10.1109/TEMSCON.2017.7998366.

[5] M. M. Garcia and S. Hawes, “Africa Energy Outlook 2019,” Energy Outlook, 2021, [Online]. Available: https://webstore.iea.org/africa-energy-outlook-2019.

[6] Department of Minerals and Energy, “Energy Efficiency Strategy of the Republic of South Africa Department of Minerals and Energy March 2005 Foreword,” Africa (Lond)., no. April, p. 44, 2005.

[7] W. Hart Danial, Power Electronics. Indiana: McGraw-Hill, 2011.

[8] R. Haider, R. Alam, N. B. Yousuf, and K. M. Salim, “Design and construction of single phase pure sine wave inverter for photovoltaic application,” 2012 Int. Conf. Informatics, Electron. Vision, ICIEV 2012, pp. 190–194, 2012, doi: 10.1109/ICIEV.2012.6317332.

[9] S. Gao and M. Barnes, “Phase-locked loops for grid-tied inverters: Comparison and testing,” IET Conf. Publ., vol. 2016, no. CP684, 2016, doi: 10.1049/cp.2016.0304.

[10] V. C. Kotak and P. Tyagi, “DC To DC Converter in Maximum Power Point Tracker,” pp. 6115–6125, 2013.

[11] B. P. Singh, S. K. Goyal, and S. A. Siddiqui, “Grid Connected-Photovoltaic System (GC-PVS): Issues and Challenges Grid Connected-Photovoltaic System (GC-PVS): Issues and Challenges,” 2019, doi: 10.1088/1757-899X/594/1/012032.

[12] M. A. Omar and M. M. Mahmoud, “Design and Simulation of a PV System Operating in Grid-Connected and Stand-Alone Modes for Areas of Daily Grid Blackouts,” vol. 2019, 2019.

[13] L. Hadjidemetriou, “Synchronization and Control Methods for grid-connecting Renewable Energy Sources,” pp. 1–51,Apr. 2015.

[14] S. Pal and K. B. Sahay, "Modeling of Solar Energy Grid Integration System Using Typhoon HIL," 2018 Int. Electr. Eng. Congr., vol. 1, pp. 1–5, 2018.

[15] S. Yasmeena and G. T. Das, "A Review of Technical Issues for Grid Connected Renewable Energy Sources," Int. J. Energy Power Eng. Int. J. Energy Power Eng. Spec. Issue Energy Syst. Dev., vol. 4, no. 5, pp. 22–32, 2015, doi: 10.11648/j.ijepe.s.2015040501.14.

[16] Y. Jiang, Y. Li, and Y. Tian, "Phase-Locked Loop Research of Grid-Connected Inverter Based on Impedance Analysis," 2018, doi: 10.3390/en11113077.

[17] R. Izah and D. Prastiyanto, "Improvement of DSOGI PLL Synchronization Algorithm with Filter on Three-Phase Grid-Connected Photovoltaic System," vol. 18, no. 1, pp. 35–45, 2018.

[18] Y. Yang et al., "Benchmarking of Phase Locked Loop based Synchronization Techniques for Grid-Connected Inverter Systems," pp. 2167–2174, 2015.

[19] J. Ögren and J. Ögren, "PLL design for inverter grid connection Simulations for ideal and non-ideal grid conditions," 2011.

[20] P. S. A. Survey, E. Rakhshani, K. Rouzbehi, J. S. Adolfo, and A. C. Tobar, "Integration of Large Scale PV-Based Generation into."

[21] S. M. Tripathi and S. Singh, "Hardware-in-the-Loop Simulation of Grid-tied Converter for Unity Power Factor Operation," no. 4, pp. 250–253, 2020, doi: 10.1109/IC3A48958.2020.233669.

[22] P. Inverters and T. M. Techniques, "and Control Strategies," 2020.